Propofol-induced Sedation Diminishes the Strength of Frontal-Parietal-Occipital EEG Network

Dheeraj Rathee*, Hubert Cecotti *Senior Member, IEEE*, Girijesh Prasad *Senior Member, IEEE*

***Abstract*— The level of conscious experience can be effectively and reversibly altered by the administration of sedative agents. Several studies attempted to explore the variations in frontal-parietal network during propofol-induced sedation. However, contradictory outcomes warrant further investigations. In this study, we implemented the Neural Gas algorithm-based delay symbolic transfer entropy (NG-dSTE) for investigation of frontal-parietal-occipital (F-P-O) network using scalp EEG signals recorded during altered levels of consciousness. Our results show significant disruption of the F-P-O network during mild and moderate levels of propofol sedation. In particular, the interaction between frontal and parietal-occipital region is highly disturbed. Moreover, we found measurable effect of sedation on local interactions in the frontal network whereas parietal-occipital network experienced least variations. The results support the conclusion that the connectivity based features can be utilized as reliable biomarker for assessment of sedation levels effectively.**

I. INTRODUCTION

The number of non-invasive and minimally invasive procedures performed outside of the operating room has grown exponentially over the last decade. Sedation, analgesia or both may be needed for many of these interventional or diagnostic procedures. Several scientific studies and clinical surveys have confirmed the strong association between excessive and/or insufficient sedation and negative healthcare outcomes [1]. Additionally, correct assessment of sedation during intensive care unit (ICU) stay may result in substantial decrease in mortality, mechanical ventilation, duration of stay, improved healthcare resource employment, and decreased overall healthcare cost [1], [2].

The process of reversibly inducing unconsciousness using anaesthetic drugs like propofol is a commonplace in clinical medicine. Several studies have reported propofol-induced changes in the fronto-parietal associative brain networks [3], [4], [5], [6]. The majority of them involve functional MRI-based analysis for functional connectivity networks while only a few studies include EEG signals for their analysis. Though fMRI exhibits high spatial resolution, its application for assessment of sedation in clinical settings poses several challenges. For instance, there exits a high susceptibility to artifacts produced due to head movements. Nevertheless, the effect of propofol on the fronto-parietal network is still unclear. Moreover, a recent study argued about the significant role of the occipital region in maintenance of conscious experience [7].

Estimating connectivity between different brain regions using electroencephalography (EEG) is a popular alternative to study the causal communication mechanisms between distinct neuronal systems [8], [9]. However, the process is a non-trivial task, with several potential problems caused by inner characteristics of the EEG signals and the limitations of the connectivity methods employed. Broadly, these methods have been classified as being measures of either functional or effective connectivity [10]. The main difference between functional and effective connectivity is that the latter quantifies the directional influences at the neuronal level, while the former measures the statistical covariation between signals recorded in different brain regions. Effective connectivity measures can be further categorized as model-based approaches including dynamical causal modelling (DCM) [11] and granger causality (GC) [12], and information-theoretic approaches including mutual information (MI), and transfer entropy (TE) [13]. The application of DCM is restricted by the requirement of a priori information about potential connectivity configurations, while GC measure may provide spurious findings as a result of its linear interpretation, sensitivity to noise and band pass filtering [14].

Recently, TE has drawn wide attention among neuroscientists [15], [16]. It is an information-theoretic measure, originally introduced by Schreiber [13], and has often been used to estimate directional information flow among distinct brain regions. Several algorithms have been developed for estimating TE, however, Kraskov and Grassberger algorithm [15] is the most popular. The robustness and accuracy of this measure was found superior when applied to time-series data from linear and nonlinear models with unidirectional and bidirectional interactions. It was initially presented for estimating mutual information (MI) in [15] and later extended to compute TE. As with most of the related techniques, estimation of TE requires great amounts of data, fine-tuning of parameters and becomes vulnerable in the presence noise. Alternatively to TE, the symbolic representation of original time-series facilitates the use of a variety of powerful techniques that allow a convenient treatment of dynamics. In the case of multichannel EEG recordings, where the complex system dynamics are densely sampled and correspond to activations from distributed brain networks [17], a multichannel symbolization scheme is desired. Recently, a neural-gas (NG) algorithm based multivariate symbolization scheme for TE estimation has been

D.R. was supported by Ulster University Vice Chancellor's Research scholarship (VCRS). G.P. and H.C. were supported by the NIFBM Facility project (1303/101154803). G.P. was also supported by the UKIERI DST Thematic Partnership project (UKIERI-DST-2013-14/126).

D.R., H.C. and G.P. are with the Intelligent Systems Research Centre, School of Computing & Intelligent Systems, Ulster University, Derry∼Londonderry, N. Ireland, UK. Corresponding author: Dheeraj Rathee: rathee-d@email.ulster.ac.uk

proposed [16]. The study displayed superior performance of NG-based delay symbolic transfer entropy (*NG-dSTE*) as compared to other conventional methods for both simulated and experimental data.

To better understand the factors underlying the alterations in the EEG scalp network, we estimated and analyzed directional interactions between the EEG signals from frontal, parietal, and occipital electrodes of healthy volunteers sedated with Propofol. The different levels of sedation were determined based on the drug concentrations in blood and the objective assessment of behavioral responsiveness. The remainder of this paper proceeds as follows: Section II describes the methodology, EEG dataset, and the data analysis steps. Next, Section III presents the overall results. Finally, Section IV discusses and summarizes the findings of this study.

II. Material and Method

A. EEG Dataset

The dataset includes artefact cleaned, 91 channels, eyes-closed resting state EEG recordings from 20 healthy participants (9 male; 11 female) (mean age = 30.85; SD = 10.98). The data were recorded at four different levels of consciousness (i.e., awake, mild, moderate, and recovery) achieved by varying blood concentrations of propofol. The preprocessing steps involved artefact removal, bandpass filtering (0.5-45Hz) and segmentation (10 s non-overlapping). A mean (SD) of 38 (5), 39 (4), 38 (4) and 40 (2) epochs were obtained for awake, mild, moderate and recovery states, respectively. The details of the experimental protocol are described in [18]. In the current study, EEG data from seven participants were analyzed as the behavioral response analysis suggested significant variations in their responses with different blood concentrations of propofol. EEG was measured in microvolts (μV), sampled at 250 Hz and referenced to the vertex, using the Net Amps 300 amplifier (Electrical Geodesics Inc., Eugene, Oregon, USA). The dataset is freely available from the University of Cambridge Data Repository (https://www.repository.cam.ac.uk/handle/1810/252736).

B. Neural-Gas delayed Symbolic Transfer Entropy (NG-dSTE)

Estimation of *NG-dSTE* based connectivity measure is a two-step process [16]. The first step involves transcribing the temporal dynamics from any pair of sensors into two distinct symbolic time-series that share a common set of symbols (i.e., codebook). The size and content of the codebook depend on the temporal information present in the data. The second step involves the estimation of the delayed transfer entropy based on the symbolic time-series obtained in the first step.

Let's assume two time-series ${}^{A}Y_t$ and ${}^{B}Y_t$ from a pair of channels A and B of size T. Their corresponding time-delay vectors can be reconstructed as $U_n = [y_i, y_{i+\tau}, ..., y_{i+(\lambda-1)\tau}]$, where λ is the embedding dimension, τ denotes the embedding time delay and $n \in \{1, ..., T-(\lambda-1)\tau\}$. The two individual sequences of time-delay vectors are collectively gathered to a common reconstructed state space by forming the overall data matrix: ${}^{AB}Z = [{}^{A}U; {}^{B}U]$. Further, a codebook consisting of k code vectors is designed by applying the NG algorithm to the data matrix ${}^{AB}Z$. The NG algorithm is an unsupervised artificial neural network model, which converges efficiently to a small number $k << T$ of codebook vectors $\{M_i\}_{i\in\{1,...,k_o\}}$ using stochastic gradient descent procedure with a soft-max adaptation rule that minimizes the average distortion error [19].

The optimal value of k (i.e. k_o) for efficiently symbolizing the data matrix can be obtained by implementing a minimum distortion error scheme [15]. At the vector-quantization phase, each vector of ${}^{A}U$ and ${}^{B}U$ is assigned (according to the nearest-prototype rule) to the most similar prototype among the derived code-vectors $\{M_i\}_{i\in\{1,...,k_o\}}$. This step completes the mapping of original time-series to two symbolic time-series ${}^{A}S_n$ and ${}^{B}S_n, n \in \{1, ..., T-(\lambda-1)\tau\}$, which can be formally defined as follows:

$$
\begin{aligned}
{}^{A}U_n \overset{NG}{\rightarrow} M_{j_1} \in \{M_i\}_{i=1}^{k_o}, \{M_i\} \in \Re^{\lambda} \\
{}^{B}U_n \overset{NG}{\rightarrow} M_{j_2} \in \{M_i\}_{i=1}^{k_o}, \{M_i\} \in \Re^{\lambda} \\
{}^{A}U_n \rightarrow {}^{A}S_n = j_1(n), {}^{B}U_n \rightarrow {}^{B}S_n = j_2(n)
\end{aligned}
$$

where j_1 and $j_2 \in \{1, ..., k_o\}$. Given a pair of symbolic sequences ${}^{A}S_n$ (symbolic sequence of signal A) and ${}^{B}S_n$ (symbolic sequence of signal B) the relative frequency of symbols can be used to estimate joint and conditional probabilities, and to define *dSTE* as follows:

$$
\begin{aligned}
dSTE_{BA} = \sum p({}^{A}S_{n+1}, {}^{A}S_n, {}^{B}S_{n+1-\delta}). \\
\log \frac{p({}^{A}S_{n+1} | {}^{A}S_n, {}^{B}S_{n+1-\delta})}{p({}^{A}S_{n+1} | {}^{A}S_n)}
\end{aligned} \tag{1}
$$

where δ is the delay time between the driving and the driven system. The log is with base 2, thus $dSTE_{BA}$ is given in bits. The formulation of TE with a time delay was first proven to be effective in a recent study, which presented a robust method for neuronal interaction delays [20].

C. Data Analysis

The majority of connectivity methods are sensitive to volume conduction, thus the first step of data processing involved the estimation of current source densities (CSD) using spherical spline method [21]. A recent study showed that surface Laplacian estimation improves the interpretability of connectivity results by reducing the amount of spurious interactions [22]. Further in the analysis, we investigated eight scalp electrodes including frontal (FP1, FP2, F3, F4), parietal (P3, P4), and occipital (O1, O2) areas of the brain. The EEG data were bandpassed in the 8-12 Hz frequency band as our preliminary investigation showed significant changes specifically in alpha band only [23]. Bandpass filtering was applied by employing an 4^{th} order, zero-phase forward and backward bandpass Butterworth filter. *NG-dSTE* connectivity measures were estimated for each 10 s epoch

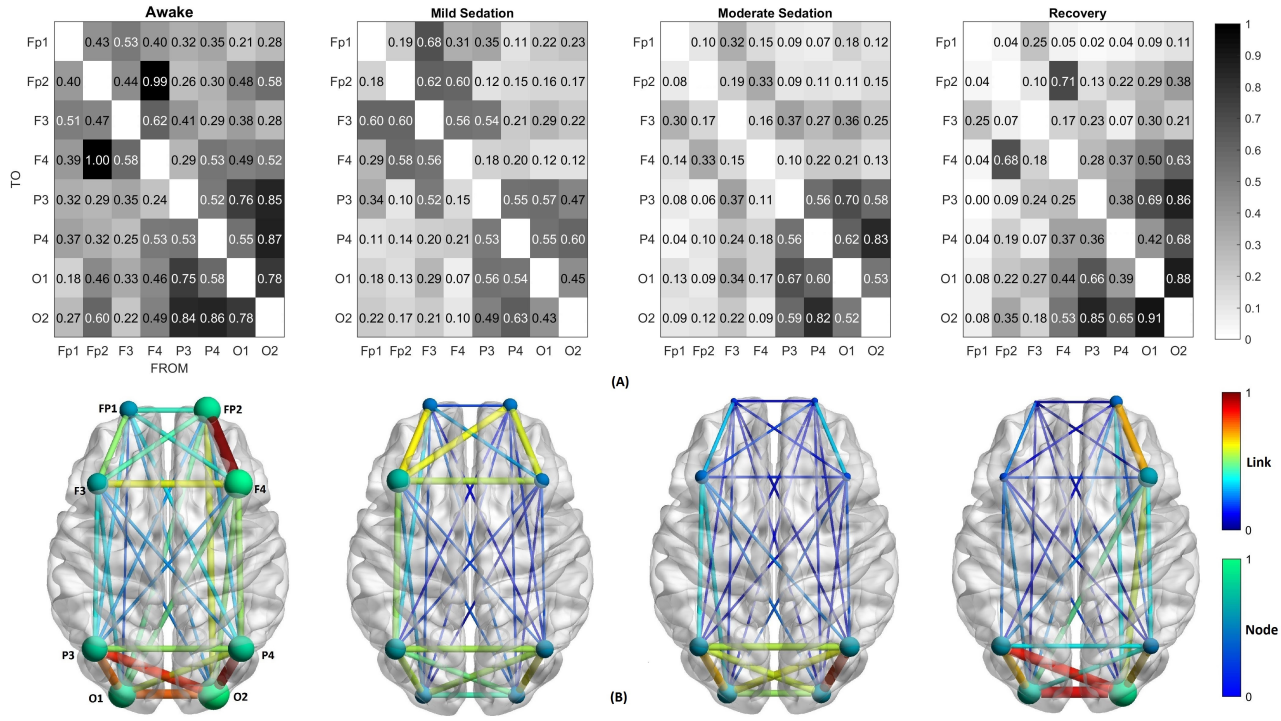

Fig. 1. (A) Normalized directed connectivity graphs (G_d) for awake, mild, moderate, and recovery states. Each cell of the matrices represents directional connectivity strength ($dSTE$) from corresponding j^{th} column electrode (From/Source) to i^{th} row electrode (Destination/Sink). (B) Scalp connectivity networks in the four states with each link representing the average information flow between two electrodes (i.e., link strength=mean($dSTE_{ij}$,$dSTE_{ji}$)) and the node strengths provide the sum of all the corresponding incoming and outgoing $dSTE$ values.

for all four states and seven subjects. Three embedding parameters, embedding dimension (λ), embedding delay (τ), and delay time (δ), are needed for *NG-dSTE*. We adopted Ragwitz criterion for optimizing the embedding dimension λ and the embedding delay τ [24]. The parameter λ and τ were ranging from 6 to 8 and 3 to 5, respectively, for the entire set of subjects and the different conscious states. Further, for each pair of time series, both way *NG-dSTE* values were estimated for a range of time lags ($1 \leq \delta \leq 0.5 \times$(epoch length in s)) and the time lag corresponding to maximum value of joint dSTE was considered. Finally, to eliminate the statistical biasness and detection of significant causal interactions, permutation resampling test was used with 1000 iterations. The null hypothesis was considered to be rejected with $p \leq 0.01$ (Bonferroni corrected for multiple comparisons). These processing steps were implemented using custom Matlab (V8.6) scripts on a Intel Core i7-4790 processor with 16 gb of memory.

III. Results

The data processing and analysis yielded 56 effective connectivity features per segment and per state. In addition, the permutation testing provided p-values for each connectivity feature. Thus, sparse networks were generated by removing the non-significant causal interactions and the remaining features were averaged across segments to generate a single directed connectivity graph (G_d) for each state.

Fig. 1(A) presents G_d graphs in form of matrices with gray scale color coding and normalized values of *dSTE* measures.

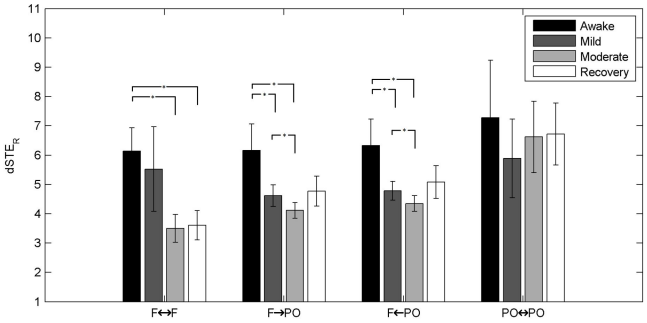

Fig. 2. Average region-wise dSTE estimates ($dSTE_R$) for four different networks i.e., within frontal (F↔F), within Parietal-Occipital (PO↔PO), Frontal to Parietal-Occipital (F→PO), and Parietal-Occipital to Frontal (F←PO) and four conscious states. The error bar represents the standard error across 7 subjects ($^*p < 0.05$, FDR corrected).

Furthermore, we estimated the node strengths ($Node_s$) for all electrodes by taking the sum of all the associated directed connectivity (i.e. both incoming and outgoing). Fig. 1(B) illustrates the frontal-parietal-occipital network as ball-and-stick models. The sizes of the nodes are assigned with a normalized value for the nodal strength and links between the nodes represents the average information transfer between them. We found a gradual reduction in the dSTE values as well as node strengths during the transition of conscious states from awake to moderate whereas during recovery state information flow regained in most of the regions, notably in Parietal-Occipital (PO) area (see Fig. 1). However, PO

TABLE I

SIGNIFICANT DIRECTED CONNECTIVITY MEASURES FOR INTER-STATE COMPARISONS (P<0.05, FDR CORRECTED). "↔" AND "→" REPRESENT BI-DIRECTIONAL AND UNI-DIRECTIONAL CONNECTIVITY.

Inter-state comparison	Significant connectivity measures
Awake-Mild	(FP2↔O2), (F4↔P4),(F4→O1), (O2→F4)
Awake-Mod	(FP1↔O2), (FP1↔P3),(FP1→FP2),(FP2↔O2), (FP2↔P3),(FP2↔F4),(F3↔F4), (P4→F4)
Awake-Rec	(FP1↔O2), (FP1↔P3),(FP1→FP2), (FP1→F4)
Mild-Mod	(FP1↔F3), (FP1↔P3),(FP1→O2)
Mild-Rec	(FP1↔P3), (F4↔O1), (P3→F3)
Mod-Rec	Nil

network start regaining its strength during moderate state after an initial decrease in connectivity strengths from awake to mild.

Furthermore, we performed a Wilcoxon signed rank test for pairwise comparison between different states. Directed connectivity measures which rejected the null hypothesis ($p < 0.05$, FDR corrected) during pairwise inter-state comparative analysis are provided in Table I. Next, we estimated inter and intra network strengths for Frontal and Parietal-Occipital networks ($dSTE_R$). The analysis yields four different measures i.e., within frontal (F↔F), within Parietal-Occipital (PO↔PO), Frontal to Parietal-Occipital (F→PO), and Parietal-Occipital to Frontal (F←PO). Fig. 2 presents the averaged (across subjects) values of these measures during the four states. The statistical comparison showed significant variations in F↔F network strength between awake vs moderate and awake vs recovery ($p < 0.05$, FDR corrected). Similarly, we found significant differences between awake, mild and moderate states for both F→PO and F←PO. However, none of the pairwise comparisons provided a significant difference for PO↔PO network.

IV. DISCUSSION AND CONCLUSION

The role of frontal-parietal network in maintenance of consciousness has been unclear because of several contradictory findings. A recent study assessing directional connectivity with GC did not find a decrease of connectivity after propofol-induced unconsciousness [25] whereas several other studies showed significant decrease in the frontal-parietal network [3], [6]. In this study, we analyzed four different subsets of frontal-parietal-occipital network using NG-based STE. Our analysis yielded several findings. First, we observed a significant disruption of both frontal to parietal, parietal to frontal connectivities during propofol-induced sedation. A similar pattern has been reported previously between awake and fully anesthetized subjects [3]. Second, the frontal network also showed similar reduction pattern but failed to discriminate between awake and mild states. Finally, local information flow in parietal-occipital network informed least about the level of sedation. Future work will include investigation of the dynamics of EEG based connectivity networks during altered levels of sedation.

REFERENCES

[1] L. M. Aitken and A. P. Marshall, "Monitoring and optimising outcomes of survivors of critical illness," *Intensive Crit. Care. Nurs.*, vol. 31, no. 1, pp. 1–9, 2015.

[2] Y. Shehabi *et al.*, "Sedation depth and long-term mortality in mechanically ventilated critically ill adults: a prospective longitudinal multicentre cohort study," *Intensive care Med.*, vol. 39, no. 5, pp. 910–918, 2013.

[3] G. Gürkan *et al.*, "Analysis of brain connectivity changes after propofol injection by generalized partial directed coherence," *Digital Signal Processing*, vol. 25, pp. 156–163, 2014.

[4] P. Guldenmund *et al.*, "Propofol-induced frontal cortex disconnection: A study of resting-state networks, total brain connectivity, and mean BOLD signal oscillation frequencies," *Brain Conn.*, vol. 6, no. 3, pp. 225–237, 2016.

[5] P. Barttfeld *et al.*, "Factoring the brain signatures of anesthesia concentration and level of arousal across individuals," *Neuroimage: Clinical*, vol. 9, pp. 385–391, 2015.

[6] M. Papadopoulou *et al.*, "Estimating directed connectivity from cortical recordings and reconstructed sources," *Brain Topogr.*, pp. 1–12, 2015.

[7] C. Koch *et al.*, "Neural correlates of consciousness: progress and problems," *Nature Rev. Neurosci.*, vol. 17, no. 5, pp. 307–321, 2016.

[8] D. Rathee *et al.*, "Estimation of effective fronto-parietal connectivity during motor imagery using partial granger causality analysis," in *Proc. Int. Joint Conf. Neural Netw. (IJCNN)*. IEEE, 2016, pp. 2055–2062.

[9] V. Youssofzadeh *et al.*, "Directed functional connectivity in fronto-centroparietal circuit correlates with motor adaptation in gait training," *IEEE Trans. Neural Syst. and Rehabil. Eng.*, vol. 24, no. 11, pp. 1265–1275, 2016.

[10] K. J. Friston, "Functional and effective connectivity: a review," *Brain Conn.*, vol. 1, no. 1, pp. 13–36, 2011.

[11] K. J. Friston *et al.*, "Dynamic causal modelling," *Neuroimage*, vol. 19, no. 4, pp. 1273–1302, 2003.

[12] C. W. Granger, "Investigating causal relations by econometric models and cross-spectral methods," *Econometrica*, pp. 424–438, 1969.

[13] T. Schreiber, "Measuring information transfer," *Phys. Rev. Lett.*, vol. 85, no. 2, p. 461, 2000.

[14] H. Nalatore *et al.*, "Mitigating the effects of measurement noise on granger causality," *Phys. Rev. E*, vol. 75, no. 3, p. 031123, 2007.

[15] A. Kraskov *et al.*, "Estimating mutual information," *Phys. Rev. E*, vol. 69, no. 6, p. 066138, 2004.

[16] S. Dimitriadis *et al.*, "Revealing cross-frequency causal interactions during a mental arithmetic task through symbolic transfer entropy: a novel vector-quantization approach," *IEEE Trans. Neural Syst. and Rehabil. Eng.*, vol. 24, no. 10, pp. 1017–1028, 2016.

[17] Y. K. Meena *et al.*, "Towards increasing the number of commands in a hybrid brain-computer interface with combination of gaze and motor imagery," in *Proc. 37th Annual Int. Conf. EMBC*. IEEE, 2015, pp. 506–509.

[18] S. Chennu *et al.*, "Brain connectivity dissociates responsiveness from drug exposure during propofol-induced transitions of consciousness," *PLoS Comput Biol*, vol. 12, no. 1, p. e1004669, 2016.

[19] T. M. Martinetz *et al.*, "'neural-gas' network for vector quantization and its application to time-series prediction," *IEEE Trans. Neural Net.*, vol. 4, no. 4, pp. 558–569, 1993.

[20] M. Wibral *et al.*, "Measuring information-transfer delays," *PloS one*, vol. 8, no. 2, p. e55809, 2013.

[21] F. Perrin *et al.*, "Scalp current density mapping: value and estimation from potential data," *IEEE Trans. Biomed. Eng.*, vol. 4, pp. 283–288, 1987.

[22] M. X. Cohen, "Comparison of different spatial transformations applied to EEG data: A case study of error processing," *Int. J. Psychophysiol.*, vol. 97, no. 3, pp. 245–257, 2015.

[23] D. Rathee *et al.*, "Effective connectivity analysis in fronto-centro-parietal network during altered levels of consciousness," *Front. Neuroinform.*, no. 58, 2016.

[24] M. Ragwitz and H. Kantz, "Markov models from data by simple nonlinear time series predictors in delay embedding spaces," *Physical Review E*, vol. 65, no. 5, p. 056201, 2002.

[25] A. B. Barrett *et al.*, "Granger causality analysis of steady-state electroencephalographic signals during propofol-induced anaesthesia," *PloS one*, vol. 7, no. 1, p. e29072, 2012.